高压空气环境下 TIG 焊接机器人关键技术

薛 龙, 王中辉, 周灿丰, 焦向东
(北京石油化工学院 光机电装备技术北京市重点实验室, 北京 102617)

摘 要: 针对渤海湾石油管道的技术特点和项目内容要求, 研制出一种在 60~100 m 深的水域完成输油管道的修补作业的水下高压全位置焊接的焊接机器人。使用 PPI 通信协议, 控制系统实现多机工作的协调和管理, 解决了对机器人的运动参数的控制和焊接参数的接管控制。采用人机交互系统, 实现了对机器人的控制和对焊接状态、场景的监控, 同时解决了高压环境下的无人操作自动焊接问题。在 0.1 MPa, 0.3 MPa, 0.5 MPa 和 0.7 MPa 压力下, 进行 16Mn 试件的焊接工艺研究, 获得良好的单面焊双面成形的效果。试验研究表明, 提高焊接机器人的控制水平、采用遥控操作, 是解决高压干式焊接的关键技术。

关键词: 水下管道; 高压干式焊接; 电弧; 焊接机器人
中图分类号: TG456.5 文献标识码: A 文章编号: 0253-360X(2006)12-017-04

薛 龙

0 序 言

早在 20 世纪 50 年代, 美国就开展了水下管道维修技术和机具的研究, 到了 20 世纪 70 年代, 随着海上油气田的开发转向深水海域, 国外石油公司相继开发了深水管道的维修技术和设备。

在陆地管道工程建设施工中, 主要的手段仍然是焊接。那么水下管道的维修, 自然首选焊接这一成熟的技术手段。水下焊接维修法是在水下环境中进行的焊接作业, 水下焊接修补主要有 3 种方法, 即, 水下湿法焊接、水下局部干法焊接和水下干式焊接。近年来, 又出现了水下摩擦叠焊、等离子焊等新方法[1~5]。

在水下管道维修的高压干式焊接施工作业中, 目前国外多采用高压轨道式 TIG 焊接系统进行, 较为知名的作业系统有 OOTO 系统、PRS 系统及 THOR21 系统等[6~9]。OOTO 系统由英国 Aberdeen Subsea Offshore Ltd. 开发, 其核心部分是焊接接头和轨道, 还包括电气控制部分、气体供应室、焊接监控室和潜水监控室等, 整个系统采用光纤传导和计算机进行监控。在高压舱中配备潜水员, 主要是为了更换电极、调整送丝角度和位置, 一旦焊接过程开始, 就不再需要潜水员干预。PRS 系统由挪威 Statoil 公司组织开发, 所涉及的研究单位包括英国 Isotek 公司、挪威 SINTEF、挪威 Norsk Hydro 等单位。该系统的设计目标是能从事 1 000 m 水深处的焊接, 施工全过程由计算机控制完成; 水面和水底之间的通讯系统由水面 PC 机和水底微处理器组成, 在焊接接头两侧安装有送丝装置和摄像头, 可以上行焊接和下行焊接; 预热、调整、退磁及保护气体输送等全部准备工作由水面焊接控制室遥控, 在潜水员手工辅助下完成。在结合不同水深针对该系统各个模块进行广泛测试的基础上(最深达 334 m), 1994 年秋季, 将该系统首次用于 Troll 近海项目中。国内海洋石油和天然气的勘探和开发起步较晚, 与国外相比, 在技术、设备等方面仍有不小的差距, 几乎还没有能够实施水下管线维修的作业装置, 相应水下管线的维修工作几乎都是委托给国外的工程公司进行, 费用昂贵。

收稿日期: 2005-10-14
基金项目: 国家 863 高技术研究发展计划资助项目(2002AA602012); 光机电装备技术北京市重点实验室开放课题(KF05-02); 北京市属市管高等学校人才强教计划资助项目

1 水下高压 TIG 焊接机器人总体设计

1.1 水下高压焊接机器人技术要求

根据渤海石油管道的技术特点和项目的内容要求, 在 60~100 m 深的水域完成输油管道的修补作业, 焊接由水面焊接专家遥控指导, 经过初步焊接专业培训的潜水员在高压舱中只完成更换钨极、姿态调整等简单辅助操作工作, 关键核心工作由焊接机器人自动完成, 因而要求焊接机器人有很高的控制水平、可靠性、可操作性和安全操作性。

1.2 水下高压焊接机器人系统总成

根据要求和国外相对研究比较成熟经验，研制一套 TIG 焊接机器人，其系统主要构成有焊接行走小车、钨极高度自动调节器、钨极横向自动调节器、钨极二维精细调准器、焊接摆动控制器、遥控盒、送丝机构、导轨、TIG 焊接电源、TIG 焊炬、水冷系统、气体保护系统、弧长控制器、角度检测器、场景监视系统、控制箱等部分组成。为保证施工现场安全，所有驱动电机均采用 24 V 直流伺服电机或步进电机。要求行走机构采用变位调节装置，可以方便适应直导轨和圆导轨的焊接要求。

1.3 水下高压焊接机器人系统空间配置

根据美国 API 有关规范的要求：干式舱内只提供 36 V 低压电，按照“水下干式管道维修系统”干式舱总体设计方案，需要将研制的焊接系统设备分开放置，即高压焊接电源及其控制计算机、保护气瓶放置在支持母船上，轨道焊机及其控制器、送丝机放置在干式舱内，二者之间通过长 100 m 的焊接专用脐带相连。

焊接专用脐带传送焊接过程所需要的电力、气体和控制信号，并将有关的焊接数据传输到焊接电源控制计算机。焊接专用脐带设计由 14 根缆管组成，其中焊接电缆 4 根，送丝机控制信号线缆 2 根，AVC 控制信号线缆 1 根，弧压反馈信号线缆 1 根，焊接电流反馈信号线缆 1 根，焊机位置（角度）反馈信号线缆 1 根，保护气管 3 根，焊接电弧视频信号线缆 1 根。控制信号线缆与反馈信号线缆设计充分考虑备用、选择双层屏蔽双绞线解决信号传输损失和干扰等。

干式舱内的焊接由舱内潜水员使用轨道自动焊机完成，潜水员不直接控制焊接电源，而是通过声讯系统与支持母船上的焊接监督工程师实现信息交流，焊接监督工程师掌握焊接过程信息的另一个重要手段是参考焊接电源控制计算机上显示的焊接电流、电弧电压以及轨道焊机位置信号。

支持母船上 TIG 焊接电源的电力供应是通过 440 V/380 V 三相变压器来实现的，干式舱内与焊接有关的设备供电则是由水下分线箱 AC36 V 转换输出来实现，提供 2 路 DC±12 V、2 路 VDC ±5 V、2 路 DC24 V，为轨道焊机控制器、送丝机、焊机驱动直流电机以及焊机控制电机和传感器供电。

2 水下高压焊接机器人控制系统设计

2.1 元器件选择

由于水下油气管道修补技术复杂，施工成本高、难度大，要求相应的焊接设备自动化程度高、可靠性和可操作性高，对于所研制的水下高压 TIG 焊接机器人，控制器选用西门子可编程控制器，各种伺服驱动器及传感器均选用成熟的国际知名品牌的产品。

2.2 控制系统功能构成

水下油气管道焊接修补施工方案是由焊接专家在支撑母船上监控操作焊接，非焊接专业的潜水员在高压舱内辅助焊接机器人实施焊接，这样要求焊接机器人的自动化程度较高，能够实现管道的全位置焊接。其控制系统功能构成见图 1。

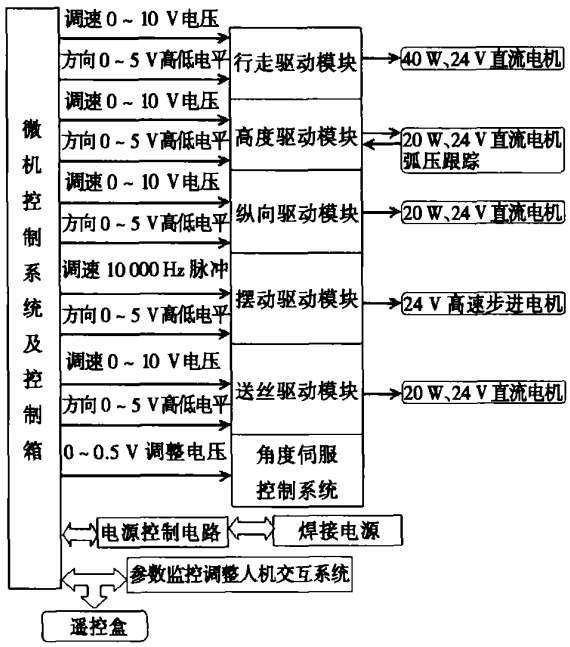

图 1 水下高压 TIG 焊接机器人系统方框图

Fig. 1 Block diagram of hyperbaric all-position TIG welding robot system

控制系统对运动参数的伺服控制，如行走小车的全位置的速度伺服控制、钨极高度的设定和弧压跟踪的自动调节控制、钨极横向的自动调节器和手动的调节控制、钨极二维精细调准控制、焊接的 4 种摆动方式的设定和摆动控制、送丝机的设定和恒速控制。

控制系统对焊接参数的控制，通过电源控制电路接口板，接管 TIG 焊接电源，实现对 TIG 焊接电源的焊接方式、焊接电流、脉冲频率与占空比、接触引弧、水冷系统、气体保护系统等控制。

控制系统对参数监控调整人机交互系统控制，通过遥控操作盒可以实现对运动参数和焊接参数的实时设定、调整和监控参数的显示等控制，通过场景监视器可以监控焊接运行状态和焊接熔池成形状

况。

2.3　计算机的协调控制

控制系统采用多机控制管理模式如图 2 所示,选用 PPI 主—从协议,主站主要负责焊接参数和运动参数的数据管理,把高压焊接工艺试验参数存储到主站的数据管理区中,建立高压焊接专家系统,为水下高压焊接提供工艺参数,同时主站也负责工作管理。从站 1 负责机器人的运动参数控制,从主站获取运动参数和控制指令,实现管道全位置焊接的各种运动功能。从站 2 主要实现水下高压焊接机器人的人机交互功能,通过遥控器和监视器,发送焊接操作各种指令、监视焊接场景和焊接熔池。

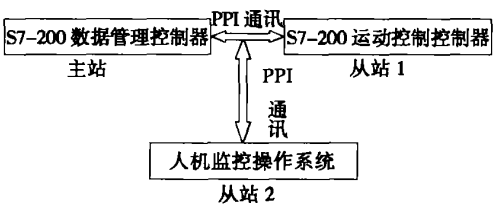

图 2　控制系统 PPI 通讯协议

Fig. 2　PPI agreement of control system

3　高压空气环境下电弧特性

3.1　高压空气环境压力对电弧电压的影响

试验条件为:电弧长度 $L=3$ mm,焊接电流 $I=130$ A,测量环境压力和电弧电压的试验数据。

由图 3 可以看出,随着环境压力的增加,电弧电压增大。由 Saha 方程知,随着环境气体压力的增加,气体的热电离度降低,电场强度增大,最终导致电弧电压增大。

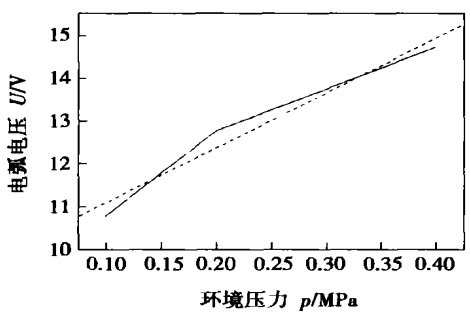

图 3　电弧电压与环境压力的关系

Fig. 3　Relations between arc voltage and environment pressure

对电弧电压与环境压力数据进行线性拟和得

$$U=9.808+12.834\ p, \tag{1}$$

式中:U 为电弧电压;p 为环境压力。

3.2　环境气体压力对电弧阴阳极压降之和与弧柱电场强度的影响

试验条件为焊接电流 $I=130$ A,测量环境压力和阴阳极压降之和、弧柱电场强度的试验数据。

由图 4 可以看出,随着环境压力的增加,电弧阴阳极压降之和增加。

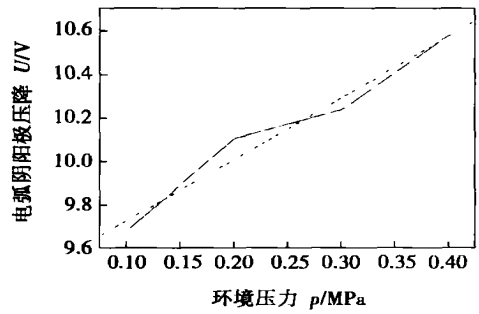

图 4　电弧阴阳极压降之和与环境压力的关系

Fig. 4　Relations between arc cathode-anode voltage and environment pressure

对阴阳极压降之和数据进行线性拟和得

$$U_{AK}=9.445+2.83\ p, \tag{2}$$

式中:U_{AK} 为电弧阴阳极压降之和;p 为环境压力。

对弧柱电场强度数据进行线性拟和得

$$E=0.32857+1.34286\ p, \tag{3}$$

式中:E 为弧柱电场强度;p 为环境压力。

由图 5 可以出看,随着环境压力的增加,弧柱电场强度增加。

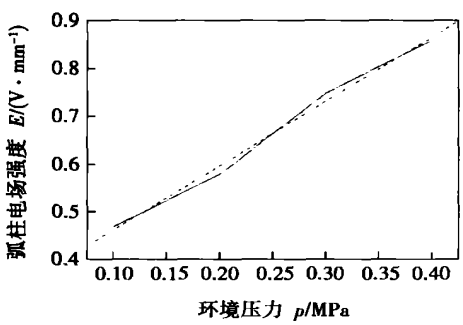

图 5　弧柱电场强度与环境压力的关系

Fig. 5　Relations between arc column electric field intensity and environment pressure

3.3　高压空气环境下的电弧静特性

试验条件为电弧长度 $L=5.5$ mm,环境压力 p 分别为 0.1 MPa, 0.2 MPa, 0.3 MPa 和 0.4 MPa,测量焊接电流和电弧电压的试验数据。

由图 6 可以看出,在一定的电弧长度下,电弧静特性曲线随气体介质压力的升高而上移。这说明在

焊接电流和电弧长度相同的条件下，在高气压下的电弧电压比在常压下高。

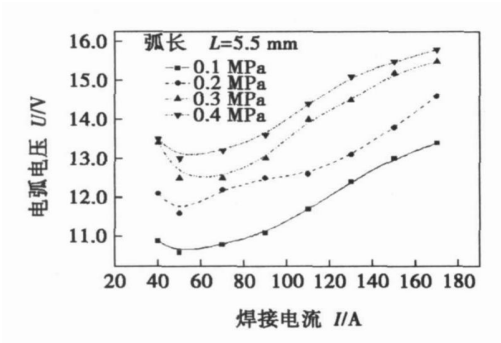

图 6 高压空气环境下氩弧的静特性曲线

Fig. 6 Static characteristic curve of TIG arc in high-pressure air condition

3.4 高压空气环境下 GTAW 电弧电压的数学模型

对试验数据进行多元线性回归，得到高压空气环境下电弧电压的数学模型为

$$U=5.3445+9.84167\,p+0.6333\,L+0.01972\,I, \quad (4)$$

式中：U 为电弧电压；p 为环境压力；L 为电弧长度；I 为焊接电流。

4 焊接工艺试验与接头力学性能

在自制的高压焊接模拟试验装置系统中进行了高压空气环境下 TIG 平板焊接工艺试验，选用合适的材料，采用合理的坡口形式，正确选择焊接方法和合理的焊接参数，在 0.1 MPa，0.3 MPa，0.5 MPa 和 0.7 MPa 压力下，对于八个位置 16Mn 试板进行焊接试验，均获得单面焊双面成形的良好效果。

试验标准是参考美国 AWS（美国焊接学会）下属的海洋结构委员会（Committee on Marine Construction）的水下焊接子委员会（Subcommittee on Underwater Welding）制定的 AWS D3.6M：1999 标准，根据 JB4708—2000 标准推荐的评定内容，开展 8 段平板不同压力下的焊接工艺试验研究。

由表1可知，不同压力下的抗拉强度都大于母材 16Mn 的抗拉强度 520 MPa，并且拉伸试件的断裂部位都在母材，可以判定，接头的拉伸试验力学性能合格。所有接头的冲击吸收功也都大于标准推荐的下限值，也是合格的。

表 1 不同压力下焊缝的力学性能

Table 1 Mechanical properties of weld in different environment pressure

环境压力 p/MPa	抗拉强度 R_m/MPa	冲击吸收功 $A_{kv(-10^\circ)}$/J
0.1	547.8	74/136/60
0.3	540.8	111/132/91
0.5	583.3	116/120/100
0.7	588	150/186/118

5 结 论

（1）研制了水下高压 TIG 焊接机器人，该机器人可靠性高、稳定性好，精度完全可以满足高压干式焊接的质量要求。

（2）对高压空气环境下的电弧特性进行了研究，随着环境压力的增加，电弧阴阳极压降之和、弧柱电场强度和电弧电压增加，电弧静特性曲线上移。建立了高压空气环境下的电弧电压数学模型，为高压空气环境下的水下焊接提供理论依据。

（3）利用自制的水下焊接机器人，进行了高压空气环境下全位置焊接工艺试验，选用合理的焊接工艺参数，实现了焊缝的单面焊双面成形，焊缝质量符合标准要求。

参考文献：

[1] 李煌英，高光军，吴 锋. 国外旧管道不停输维修技术[J]. 油气储运，2000，19(3)：53—57.

[2] 魏中格，齐雅茹，刘鸿升，等. 海底管道维修技术[J]. 石油工程建设，2002，28(4)：30—32.

[3] 宋宝天. 我国水下焊接与切割技术发展与展望[A]. 第八届全国焊接会议论文集[C]，深圳，1992，220—223.

[4] 刘 桑，钟继光，王国荣. 水下焊接技术研究与应用的新进展[J]. 中国修船，2000，6(3)：10—12.

[5] 俞建荣，张奕林，蒋力培. 水下焊接技术及其进展[J]. 焊接技术，2001，30(4)：2—4.

[6] Scott Lyons R，Middleton T B. Underwater orbital TIG welding[J]. Metal Construction，1985，5(8)：504—507.

[7] John H Nixon，Ian M Richardson. The design and construction of a 250bar hyperbaric welding research facility[J]. Materials Engineering，1995，3(2)：553—562.

[8] David Gibson，Kevin Barratt，Jan Paterson. Robotic equipment for pipeline repair[J]. Materials Engineering ASME，1995，3(2)：509—515.

[9] Dos Santos J F，Szelagowski P，Manzenrieder H. Diverless pipeline welding beyond 600 msW[J]. Materials Engineering ASME，1992，3(2)：153—163.

作者简介：薛 龙，男，1966 年出生，教授。主要研究方向为机电一体化技术和机器人技术，发表论文 40 余篇。

Email：xuelong@bipt.edu.cn

MAIN TOPICS, ABSTRACTS & KEY WORDS

Numerical simulation of welding residual stress of tube-to-tubesheet joint in heat exchangers JIANG Wen-chun, GONG Jian-ming, CHEN Hu, TU Shan-dong (College of Mechanical and Power Engineering, Nanjing University of Technology, Nanjing 210009, China). p1—4

Abstract: Using finite element program-ABAQUS, the welding residual stress of tube-to-tubesheet joint in heat exchangers had been numerically simulated. The distribution of welding residual stress was obtained. A comparison between tube end extended out of tubesheet welded joint and inside hole welded joint was made. The welding residual stress of inside hole welded joint is much smaller than that of tube end extended out of tube sheet joint. So using inside hole welded joint can decrease the susceptibility of stress corrosion cracking (SCC). The maximum of radial stress exists in the HAZ outside surface of tubesheet, which has great influence on tubesheet surface cracks. The maximum of hoop stress appears in the weld root, which has great influence on the connection failure between tube and tubesheet. The residual stress of former pipe bead is decreased due to the later pipe welding heating, which is useful for decreasing the susceptibility of SCC. This work provides a theory reference for optimizing the welding procedure and controling the welding residual stress for tube-to-tubesheet joint.

Key words: heat exchanger; tube and tubesheet; welding residual stress; finite element ABAQUS

Laser cladded Ni-based alloy coatings reinforced by nano-Sm_2O_3 particles LI Ming-xi, ZHANG Shi-hong, LI Hui-sheng, HE Yi-zhu (Research Center for Laser Processing, Anhui University of Technology, Maanshan 243002, Anhui, China). p5—8

Abstract: Ni-based alloy coatings with nano/micro-Sm_2O_3 particles addition produced by a 5 kW CO_2 laser on Q235 low carbon steel were introduced. Cross-section of the coatings was examined to reveal their microstructure using optical microscope, scanning electron microscope, and X-ray diffraction instrument. The hardness and wear resistance were measured with microhardness tester and MM200 type sliding wear machine. The results showed that γ-Ni and $Cr_{23}C_6$ exist in the coatings. Fe_7Sm, Ni_3Si and Ni_3B are also found by adding nano-Sm_2O_3. Fine microstructure and equiaxed dendrite are observed with nano-Sm_2O_3 addition. A thin layer of metallurgical bonding, the white and bright strip, is observed by adding the rare earth oxide. The hardness and wear resistance of the coatings with nano-Sm_2O_3 addition are better than that with micro-Sm_2O_3. The mechanism was found from abrasive/adhesive wear to fretting wear.

Key words: laser cladding; nano-Sm_2O_3; microstructure; microhardness; wear resistance

Movement control algorithm of automatic welding for complex intersection seam HUO Meng-you, YUE Shao-jian, WANG Xin-gang (School of Mechanical Engineering, Shandong University, Jinan 250061, China). p9—12

Abstract: On the basis of structure and principle of the five-axes linkage NC welding machine introduced in abstract, it mainly studied the movement control algorithm of the automatic welding for the complex intersection seam. Take the ellipsoidal welding conjugation tube as the example, it separately introduceal the construction of space curve equation of the intersection seam, the discrete point parameters while interpolating and fitting the intersection seam using line interpolation, the adjusting calculation of welding torch and the method of how to realize the servo control system with digital I/O board and step motor. To control automatic welding process of complex intersection seam using the software algorithm introduced, the system becomes more versatile and the cost of equipment can be decreased considerably.

Key words: automatic welding; intersection line seam; servo-control algorithm

Preliminary discussion about image character of gas pore in MAG welding based on vision sensing WANG Ke-hong, YOU Qiu-rong, SHEN Ying-ji (Department of Materials, Nanjing University Science & Technology, Nanjing 210094, China). p13—16

Abstract: A passive vision sensing system to acquire the image of molten pool in MAG welding was set up and many typical molten pool images were obtained. The relationship between the typical gas pores and the characteristics of molten pool images were studied by sync contrast experiments. Many molten pool images with surface gas pores and inner gas pores were obtained, and the change of the images and the strange characters were studied from the view of gray mean and gray standard deviation. The experiments indicate that it is feasible to judge the pores by characteristics of the vision images which offers the technological foundation for automatic identification of welding defect on the base of vision sensing. The experiments and the analysis indicate that one type of image may predicate several types of welding defect, one type of welding defect may also shows several types of image characters.

Key words: metal active-gas welding ; vision sensing; welding defect; molten pool character

Key techniques of TIG welding robot in high-pressure air condition XUE Long, WANG Zhong-hui, ZHOU Can-feng, JIAO Xiang-dong (Beijing Institute of Petro-Chemical Technology, Beijing 102617, China). p17—20

Abstract: According to the special technical features of the oil

pipelines in Bohai Sea and the requirements of the program, an all-position hyperbaric TIG welding robot for underwater pipeline recovery work in deep water of 60—100 m was developed. In its control system the harmony and management of multi-controllers was achieved by adopting PPI agreement. The parameters of command movement and that of welding movement for the welding robot were controlled. By a man-machine conversation system, the controls of the robot, welding states and scenes could be manipulated and supervised. The unmanned welding problem in hyperbaric circumstance was solved at the same time. Under the different pressures, such as 0.1 MPa, 0.3 MPa, 0.5 MP and 0.7 MPa, the welding simulations had been done with a 16Mn steel plate and the better effect of one side welding with back formation was obtained. Experimental results show that a higher control level and remote control by adoption in a robot are the key techniques of TIG welding in high-pressure air condition.

Key words: underwater pipeline; hyperbaric welding; arc; welding robot

Multimode vibration analysis of transducer in thermosonic flip chip bonding LONG Zhi-li, WU Yun-xin, HAN Lei, ZHONG Jue (College of Electromechanical Engineering, Central South University, Changsha 410083, China). p21—24, 28

Abstract: Multimode vibration of transducer and its effect on bonding quality was investigated. The velocities of different characteristic marks in the horn and bonding tool were acquired up by Laser Doppler Vibrometer. The experimental results showed that the vibration of transducer is the coupling result of different modes. The velocity ratio of non-dominant mode to dominant mode was gained. The longitudinal flexural vibration is the main non-dominant mode. This kind of longitudinal flexural vibration would "flap" the chip, influencing the bonding area, bonding strength and parallel between gold bumps and substrate. The origin of multimode in transducer was analyzed by FEM model, and some suggestions about restraining the non-dominant mode was brought forward.

Key words: multimode vibration; ultrasonic transducer; bonding quality; thermosonic flip chip bonding

Influential factors of threshold power density for Nd:YAG laser beam welding of beryllium LI Sheng-he, XIE Zhi-qiang, JIANG Yun-bo, WU Dong-zhou (China Academy of Engineering Physics, Mianyang 621900, Sichuan, China). p25—28

Abstract: Laser threshold power density of hot isometric pressure (HIP) beryllium in laser beam welding was investigated. The results show that the threshold power density was sensitive to the diameter of beryllium cylinder. It is seemed that more large diameter of beryllium cylinder, more power of back-reflection light coupling into the resonator. So more strong Q-switched pulse was formed in the cavity. Then threshold power density of HIP beryllium will decrease. For the same diameter of beryllium cylinder, when the angel of incident laser beam was adjusted from 0° to 3°, the back-reflection laser can be overcome. Threshold power density of HIP beryllium will increase. In experiment, the ratio of depth to width usually is 1.0—1.5 for deep penetration welding. However, the ratio of depth to width usually is 0.2 for heat conduction welding.

Key words: Nd:YAG laser; threshold power density; beryllium

Current-zero period process and its charcteristics of AC TIG arc HU Kun-ping, SONG Yong-lun, XIA Yuan, CHEN Zhi-xiang, (Beijing University of Technology, Beijing 100022, China). p29—33

Abstract: As an important heat source in welding, TIG arc is widely used in manufacturing industry, especially for aluminum alloy joining processes. But up to now, the knowledge concerning the alternative TIG arc during the period of the current traversing zero as well as its influence on welding process are not clear enough. Based on a modern ICCD spectral instrument and time-control statistic sampling method, the dynamic variations of electron density during the period were observed in alternative TIG welding arcs for both the square wave and sine wave. The general rules and the features of the arcs were analyzed and discussed. It may enhance the knowledge on the arc process and its control level.

Key words: alternative tunsten inert-gas arc; arc near and across zero; electron density; spectral diagnosis

Chaos characteristics of electrode displacement signals in spot welding process based on Lyapunov exponent LUO Zhen, SHANG Ping, GAO Zhan-jiao, LIU Peng-fei (School of Material Science and Engineering, Tianjin University, Tianjin 300072, China). p34—36

Abstract: Based on chaos theory and the nonlinear dynamical systems, the electrode displacement signal was studied in the spot welding process. Four quality states of spot welding were studied and the largest Lyapunov exponents are calculated. These results show that the greatest Lyapunov exponents are positive number in the four different displacement signals. According to the theory of phase space reconstruction and Lyapunov exponent, there are some chaotic characteristics in the displacement signal of spot welding and relationships between spot welding quality and Lyapunov exponent. This research provides a new method to measure and forecasting the spot welding quality.

Key word: spot welding; electrode displacement signals; Lyapunov exponent; chaos time series

Comparison of pressure characteristics between two friction welding machine hydraulic systems WANG Xi-feng[1], DU Sui-geng[1], GONG Cheng[2], YAN Nan-fei[2] (1. Key Laboratory of Ministry of Education for Contemporary Design and Integrated Manufacturing Technology, Northwestern Polytechnical University, Xi'an 710072, China; 2. Xi'an Branch of China Coal Research Institute, Xi'an 710054, China). p37—41

Abstract: In order to analyze the necessity and feasibility of close-loop process control by electro-hydranlic ration in the friction welding, the static and dynamic characteristics and the axial pressure fluctuations in long period welding production of two hydraulic systems of friction welding machine were compared. One system is con-